

Enhancement of third-order nonlinear optical susceptibilities in silica-capped Au nanoparticle films with very high concentrations

Y. Hamanaka,^{a)} K. Fukuta, and A. Nakamura^{b)}

Department of Applied Physics, Nagoya University, Nagoya 464-8603, Japan and Core Research for Evolutional Science and Technology (CREST), Japan Science and Technology Agency (JST), Tokyo 150-0002, Japan

L. M. Liz-Marzán

Department of Physical Chemistry, University of Vigo, E-36200, Vigo, Spain

P. Mulvaney

Chemistry School, University of Melbourne, Parkville, VIC, 3010, Australia

(Received 24 October 2003; accepted 15 April 2004; published online 28 May 2004; publisher error corrected 9 June 2004)

Third-order nonlinear optical susceptibilities ($\chi^{(3)}$) and response times have been investigated for silica-capped Au nanoparticles for various volume fractions, p , of Au nanoparticles ranging from 0.027 to 0.66. The imaginary part of $\chi^{(3)}$ ($\text{Im}\chi^{(3)}$) around the surface plasmon resonance increases with increasing p up to 0.34, and decreases for $p > 0.39$. In addition to the local field enhancement around the surface plasmon resonance in the composite system, an additional enhancement of $\text{Im}\chi^{(3)}$ due to the interaction between nanoparticles for $p < 0.39$ is observed.

© 2004 American Institute of Physics. [DOI: 10.1063/1.1760229]

Metal nanoparticles (NPs) embedded in dielectric materials have attracted considerable interest as active materials in nonlinear optical devices such as ultrafast optical switches.^{1–3} In the case of metal NP based composites, third-order nonlinear optical susceptibilities $\chi^{(3)}$ of 10^{-7} esu around the surface plasmon (SP) resonance and response times as short as 0.7 ps in the weak excitation limit have been observed.^{4–8} Relaxation of the nonequilibrium electron distribution generated in such metal NPs determines the ultrafast response time. In small metal NPs with a diameter less than 7 nm, breathing modes play a crucial role in determining the rate of this energy dissipation from the hot electron system to the surrounding medium.⁹

The linear optical properties of low concentrations of small spheres in a nonabsorbing medium can be quantitatively predicted by effective medium theories.^{10,11} The enhancement of $\chi^{(3)}$ has been successfully analyzed in terms of the dynamical response of the conduction electrons, provided the volume fraction p of NPs is very low.^{1,4,7} For high volume fractions, however, the mutual interaction between particles will complicate calculation of the local field and the question arises as to whether such effects will enhance or suppress the nonlinear optical response. To realize a NP composite system with high volume fractions, homogeneous NP films are needed in which there is no coalescence of the metal particles. Local field effects are extremely sensitive to small fluctuations in local geometry. Such composites were recently synthesized by coating gold NPs with thin silica shells.¹² By changing the shell thickness, the volume fraction can be systematically varied without changing the Au particle size. In this letter, we report on $\chi^{(3)}$ of silica-capped Au NP films with volume fractions varying from 0.027 to 0.66. Enhancement of $\chi^{(3)}$ up to $p = 0.34$ and damping at higher p were observed.

Spherical Au NPs encapsulated in silica shells were deposited on glass substrates.¹³ We used the same techniques of sample preparation and characterization that were used in previous reports, and the details are described in Refs. 12 and 13. The silica shell thickness was varied from 1.5 to 17.5 nm, while the diameter of Au NPs was constant (15 nm). The thinnest homogeneous silica shell that could be prepared was about 2 nm. To obtain even higher volume fractions, thinner insulating layers are needed. Higher volume fractions were achieved by using non-silica-coated Au NPs, stabilized by citrate ions (0.3 nm) and mercaptopropionic acid (1.0 nm).¹² Assuming a close-packed structure of spherical particles, p of the corresponding films varies between 0.027 and 0.66. A typical transmission electron microscopy (TEM) image of silica-capped Au NPs is shown in the inset of Fig. 1. The Au

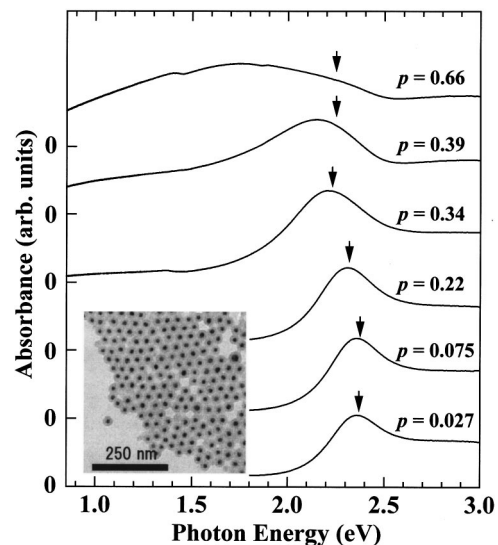


FIG. 1. Absorption spectra of silica-capped Au NP films with volume fractions of $p = 0.027$ – 0.66 . The arrows indicate the photon energies at which $|\Delta A|/(\text{Im}\chi^{(3)})$ exhibits a peak in differential absorption spectra. The inset shows a TEM image of the silica-capped Au NPs.

^{a)}Electronic mail: hamanaka@nitech.ac.jp

^{b)}Electronic mail: nakamura@nuap.nagoya-u.ac.jp

NPs are monodisperse, uniformly capped with silica shells, and completely separated from each other.

Transient absorption spectra were measured by a femto-second pump and probe method using an amplified Ti:sapphire laser system.⁹ The pump pulse energy was set to 3.1 eV (ω_{pump}) corresponding to the band-to-band transition associated with $5d$ electrons in the Au NPs. Nondegenerate components $\text{Im} \chi^{(3)}(-\omega_{\text{probe}}; -\omega_{\text{pump}}, \omega_{\text{pump}}, \omega_{\text{probe}})$ of the imaginary part of $\chi^{(3)}$ at the probe frequency of ω_{probe} ($\omega_{\text{pump}} \neq \omega_{\text{probe}}$) were deduced from differential absorption spectra measured with pump fluences of 110–460 $\mu\text{J}/\text{cm}^2$. Reflectance changes were taken into account using the values obtained from the transient reflection measurements.

Figure 1 shows absorption spectra of silica-capped Au NP films for different volume fractions. For $p=0.027$, the SP resonance band is observed at 2.36 eV. The absorption band on the higher energy side of the SP peak (>2.6 eV) corresponds to the d -band-to-Fermi level transition of electrons in the Au NPs. With an increase in p , the SP band exhibits a redshift and broadening. The spectral features change drastically at $p=0.66$, where the SP peak appears at 1.75 eV and the width of the SP band is four to five times larger than that for the lower p values. Such spectral changes indicate that interparticle interactions play a significant role in the optical response at high p . Although the spectral behavior was interpreted using Maxwell–Garnett theory in a previous report,¹³ quantitative agreement was not obtained for $p>0.3$.

Nonlinear absorption spectra and values of $\text{Im} \chi^{(3)}$ were measured using the pump and probe technique. In Fig. 2(a), we show the linear absorption spectrum of the silica-capped Au NP film with $p=0.34$ and the differential absorption spectrum (ΔA) measured with a pump fluence of 190 $\mu\text{J}/\text{cm}^2$. ΔA shows a decrease around the SP peak and an increase on both sides of the peak immediately after excitation at 3.1 eV. As the delay time is increased, ΔA decreases, but the spectral features remain constant. Using Maxwell–Garnett theory for the dielectric function of the composite system, the nondegenerate component of $\chi^{(3)}$ of metal NP composites can be represented by the third-order susceptibility $\chi_m^{(3)}$ of the bulk metal:

$$\chi^{(3)}(\omega_{\text{probe}}) = p |f_1(\omega_{\text{pump}})|^2 f_1^2(\omega_{\text{probe}}) \chi_m^{(3)}(\omega_{\text{probe}}). \quad (1)$$

Here $f_1(\omega)$ is the local field enhancement factor given by

$$f_1(\omega) = \frac{3\varepsilon_d(\omega)}{\varepsilon_m(\omega) + 2\varepsilon_d(\omega)}, \quad (2)$$

where ε_m and ε_d represent dielectric functions of the isolated metal NPs and the matrix, respectively.^{1,4} Equation (1) is applicable for $p \ll 1$, and the Maxwell–Garnett theory cannot be used for analysis of data for very high p . For the pump pulse frequency of $\omega_{\text{pump}} = 3.1$ eV, $|f_1(\omega_{\text{pump}})|$ is estimated to be ~ 1 , indicating that the local electric field of the pump pulse is not enhanced in the composite, i.e., the local field effect is important only at the probe frequency. Although this estimation is true only for $p \ll 1$, it is reasonable to assume a similar situation for very high p , because the pump pulse frequency (3.1 eV) is far from the surface plasmon resonance (<2.4 eV).

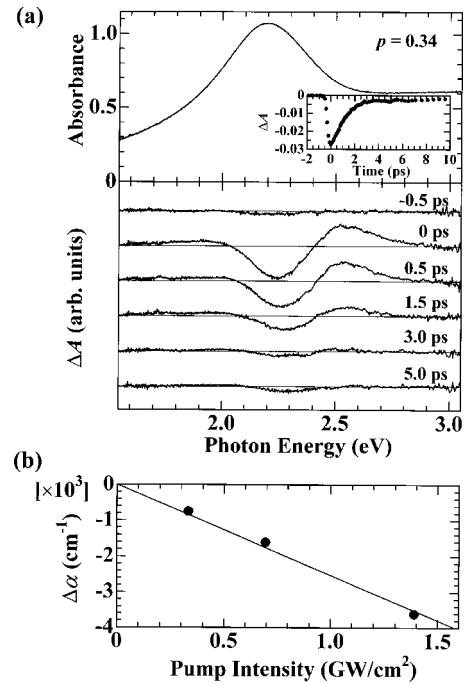


FIG. 2. (a) Absorption spectrum (upper panel) and ΔA (lower panel) measured around the SP band of the silica-capped Au NP film with $p=0.34$. The inset shows a time evolution of ΔA at 2.24 eV. (b) Change in the absorption coefficient $\Delta\alpha$ measured at 2.24 eV as a function of the pump pulse intensity. The solid line is a linear fit to the data.

For a moderate laser intensity of the pump pulse, I , the change in the absorption coefficient is described by $\Delta\alpha = \beta I$, where β is a nonlinear absorption coefficient. β is related to $\text{Im} \chi^{(3)}$ by

$$\text{Im} \chi^{(3)} = \frac{n^2 c^2}{240 \pi^2 \omega_{\text{probe}}} \beta, \quad (3)$$

where n represents the linear refractive index of the composite system at the probe frequency ω_{probe} and c is the velocity of light in vacuum.¹⁴ From the dependence of $\Delta\alpha$ on I we can estimate $\text{Im} \chi^{(3)}$ values. In Fig. 2(b), $\Delta\alpha$ values measured at 2.24 eV for $p=0.34$ are plotted as a function of the intensity of the pump pulse I . We used I values corrected for both reflection and extinction losses within the film. $\Delta\alpha$ values were estimated from the results of both the transient-transmission and transient-reflection measurements, carried out at the same pump fluence. $\Delta\alpha$ describes changes in absorption and scattering terms at ω_{probe} induced by the pump pulse. Therefore, a value of $\text{Im} \chi^{(3)}$ in the composite system includes a contribution from the scattering term in the nonlinear loss processes at ω_{probe} . As seen in Fig. 2(b), $\Delta\alpha$ decreases linearly with I . From the linear least-squares fit, β is obtained to be -2.53 cm/MW, which yields $\text{Im} \chi^{(3)}$ of -2.6×10^{-9} esu. In this estimation, we used n values that were measured from the absorption coefficient and the reflectance.¹⁵ n is ~ 1.4 for $p \leq 0.075$, and increases to ~ 3.0 at higher concentrations.

Absolute values of $\text{Im} \chi^{(3)}$ measured at the photon energies indicated by the arrows in Fig. 1 are plotted as a function of p for $p=0.027$ – 0.66 using open circles in Fig. 3. We also measured the value of $|\text{Im} \chi^{(3)}|$ for Au NPs embedded in silica glass at a very low volume fraction $\sim 10^{-4}$, and the result is shown by the closed circle in Fig. 3. $|\text{Im} \chi^{(3)}|$ is

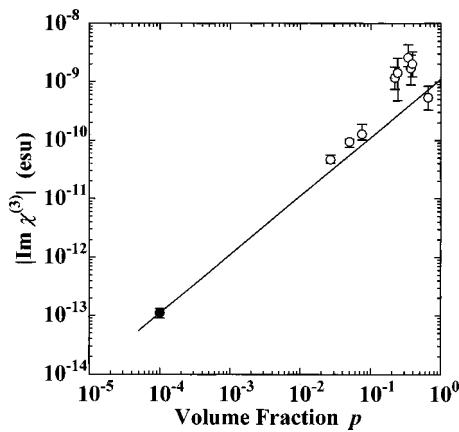


FIG. 3. Dependence of $|\text{Im } \chi^{(3)}|$ on p in silica-capped Au NP films (open circles). The value of Au NPs embedded in silica for $p=10^{-4}$ measured at 2.30 eV is also plotted (closed circle). The solid line indicates the $|\text{Im } \chi^{(3)}|$ value extrapolated from the value for $p=10^{-4}$ assuming a linear dependence on p .

$4.7(\pm 0.8) \times 10^{-11}$ esu for $p=0.027$, and reaches a maximum value of $2.6(\pm 1.3) \times 10^{-9}$ esu at $p=0.34$. At still higher metal volume fractions, $|\text{Im } \chi^{(3)}|$ decreases, slowly falling to $5.3(\pm 2.5) \times 10^{-10}$ esu at $p=0.66$.

Importantly, while there is an enhancement in $|\text{Im } \chi^{(3)}|$ at low volume fractions, the degree of enhancement in $|\text{Im } \chi^{(3)}|$ observed at high volume fractions is significantly higher, and demonstrates that in addition to the well-known local field effect, or Lorentz field contribution, coupling of SPs between particles introduces a second contribution to $\text{Im } \chi^{(3)}$. The value of $\text{Im } \chi^{(3)}$ for $p=10^{-4}$ is due solely to the enhancement by $(f_1(\omega_{\text{probe}}))^2$ compared with $\chi_m^{(3)}$ of the metal NP itself according to Eq. (1). We estimate the value of f_1^2 to be $-4.26+4.03i$, and $|f_1|^2$ is estimated to be 5.87 for the Au/silica glass composite with $p=10^{-4}$. This factor is the enhancement due to the local electric field in the low concentration limit. Extrapolating the $|\text{Im } \chi^{(3)}|$ value [$1.1(\pm 0.2) \times 10^{-13}$ esu] to the high volume fraction regime and assuming a linear dependence of $\text{Im } \chi^{(3)}$ on p , we can estimate the enhancement in $\text{Im } \chi^{(3)}$ expected from the effective medium theory. The deviation of the data from the straight line in Fig. 3 indicates the failure of the effective medium model, and is attributed to particle–particle interactions in the high p regime.¹⁶ Hence, the Maxwell–Garnett¹⁰ and Bruggemann¹¹ theories are not applicable at high p . The largest enhancement obtained was ~ 7 for $p=0.34$, which leads to an enhancement in $|\text{Im } \chi^{(3)}|$ by a factor of about 40 compared with $\chi_m^{(3)}$.

The decrease observed for $p \geq 0.39$ can be interpreted in terms of the suppression of the dielectric confinement effect. Interparticle distance between neighboring NPs is 0.6 nm for $p=0.66$. The distance for $p=0.66$ is comparable to the interatomic distance of 0.288 nm in the fcc lattice of Au crystal. Therefore, a possible explanation of the decrease in $\text{Im } \chi^{(3)}$ for $p \geq 0.39$ is a penetration effect of conduction electrons into an interface region between the NP and spacer, which suppresses the enhancement of the local electric field. Such an electron tunneling effect, however, does not lead to metallic conduction of the composite films studied here. The measured resistivities of the films are extremely high ($\sim 10^8 \Omega \text{ cm}$) even at $p=0.66$, and there is no signature of

the percolation at the critical concentration of 0.33. This result supports the contention that the Au NPs are well separated even at very high volume fractions. Liao *et al.* have studied the dependence of $|\chi^{(3)}|$ on p in Au NP/SiO₂ composites prepared by a sputtering method.¹⁷ In their sputtered films there were wide size distributions and inhomogeneities, though they observed an increase of $|\chi^{(3)}|$ at high p . The observed metallic resistivities suggest the existence of considerable coalescence of Au particles leading to metallic conduction pathways in the sputtered films.

We briefly discuss the response time of the optical nonlinearities. The time evolution of ΔA measured at 2.24 eV for $p=0.34$ is shown in the inset of Fig. 2(a). ΔA exhibited two-component decay behavior, and the relaxation time of the first component τ_1 was 1.5 ps. The measured values of τ_1 at $\sim 30 \text{ J/cm}^2$ were all found to lie in the range 1.5–1.8 ps for volume fractions ranging from $p=0.05$ to $p=0.66$. τ_1 should be determined by the electron–phonon coupling in the 15 nm gold NPs, and this process should be largely independent of p .

In summary, $\text{Im } \chi^{(3)}$ values and their response time have been investigated systematically for Au@SiO₂ composite films for volume fractions in the range from 0.027 to 0.66. We have found that the values of $\text{Im } \chi^{(3)}$ increase with increasing p , and reach a maximum value at $p \sim 0.34$ due to the further enhancement of the local field effect by particle–particle interactions, in addition to the expected increase with increasing NP concentration. For $p > 0.39$, $\text{Im } \chi^{(3)}$ decreases because of the suppression of the local field effect. The dependence of $\text{Im } \chi^{(3)}$ on p observed in this study raises the necessity for a new theoretical approach beyond the effective medium model.

¹F. Hache, D. Ricard, and C. Flytzanis, *J. Opt. Soc. Am. B* **3**, 1647 (1986).

²M. J. Bloemer, J. W. Haus, and P. R. Ashley, *J. Opt. Soc. Am. B* **7**, 790 (1990).

³R. F. Haglund, Jr., L. Yang, R. H. Magruder III, J. E. Wittig, K. Becker, and R. A. Zuhr, *Opt. Lett.* **18**, 373 (1993).

⁴K. Uchida, S. Kaneko, S. Omi, C. Hata, H. Tanji, Y. Asahara, A. J. Ikushima, T. Tokizaki, and A. Nakamura, *J. Opt. Soc. Am. B* **11**, 1236 (1994).

⁵T. Tokizaki, A. Nakamura, S. Kaneko, K. Uchida, S. Omi, H. Tanji, and Y. Asahara, *Appl. Phys. Lett.* **65**, 941 (1994).

⁶V. Halté, J.-Y. Bigot, B. Palpant, M. Broeyer, B. Prével, and A. Pérez, *Appl. Phys. Lett.* **75**, 3799 (1999).

⁷Y. Hamanaka, A. Nakamura, S. Omi, N. Del Fatti, F. Vallee, and C. Flytzanis, *Appl. Phys. Lett.* **75**, 1712 (1999).

⁸J. Olivares, J. Requejo-Isidro, R. del Coso, R. de Nalda, J. Solis, C. N. Afonso, A. L. Stepanov, D. Hole, P. D. Townsend, and A. Naudon, *J. Appl. Phys.* **90**, 1064 (2001).

⁹Y. Hamanaka, J. Kuwabata, I. Tanahashi, S. Omi, and A. Nakamura, *Phys. Rev. B* **63**, 104302 (2001).

¹⁰J. C. Maxwell-Garnett, *Philos. Trans. R. Soc. London, Ser. A* **203**, 385 (1904).

¹¹D. A. G. Bruggemann, *Ann. Phys. (Leipzig)* **24**, 636 (1935).

¹²L. M. Liz-Marzán, M. Giersig, and P. Mulvaney, *Langmuir* **12**, 4329 (1996).

¹³T. Ung, L. M. Liz-Marzán, and P. Mulvaney, *J. Phys. Chem. B* **105**, 3441 (2001).

¹⁴Y. Hamanaka, A. Nakamura, N. Hayashi, and S. Omi, *J. Opt. Soc. Am. B* **20**, 1227 (2003).

¹⁵M. J. Weber, *CRC Handbook of Laser Science and Technology, Vol. III Optical Materials Part 1* (CRC Press, Boca Raton, FL, 1986).

¹⁶A. K. Sarychev, V. A. Shubin, and V. M. Shalaev, *Phys. Rev. B* **60**, 16389 (1999).

¹⁷H. B. Liao, R. F. Xiao, J. S. Fu, P. Yu, G. K. L. Wong, and P. Sheng, *Appl. Phys. Lett.* **70**, 1 (1997).